Serviceability performance of buildings founded on rubber–soil mixtures for geotechnical seismic isolation

Tsang, Hing-Ho; Tran, Duc-Phu; Gad, Emad F.

DOI:
10.1080/13287982.2023.2230063

Publication date:
2023

Citation for published version (APA):
Tsang, H.-H., Tran, D.-P., & Gad, E. F. (2023). Serviceability performance of buildings founded on rubber–soil mixtures for geotechnical seismic isolation. *Australian Journal of Structural Engineering*, *24*(4), 265-278. https://doi.org/10.1080/13287982.2023.2230063

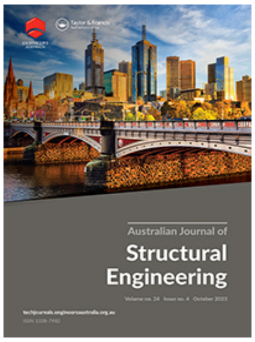

Taylor & Francis
Taylor & Francis Group

Australian Journal of Structural Engineering

ISSN: (Print) (Online) Journal homepage: www.tandfonline.com/journals/tsen20

Serviceability performance of buildings founded on rubber–soil mixtures for geotechnical seismic isolation

Hing-Ho Tsang, Duc-Phu Tran & Emad F. Gad

To cite this article: Hing-Ho Tsang, Duc-Phu Tran & Emad F. Gad (2023) Serviceability performance of buildings founded on rubber–soil mixtures for geotechnical seismic isolation, Australian Journal of Structural Engineering, 24:4, 265-278, DOI: 10.1080/13287982.2023.2230063

To link to this article: https://doi.org/10.1080/13287982.2023.2230063

AUSTRALIAN JOURNAL OF STRUCTURAL ENGINEERING
2023, VOL. 24, NO. 4, 265–278
https://doi.org/10.1080/13287982.2023.2230063

Serviceability performance of buildings founded on rubber–soil mixtures for geotechnical seismic isolation

Hing-Ho Tsang, Duc-Phu Tran and Emad F. Gad

School of Engineering, Swinburne University of Technology, Melbourne, Australia

ABSTRACT

Base isolation is a low-damage seismic design strategy that can be used for constructing resilient structures. Geotechnical seismic isolation (GSI) is a new category of emerging base isolation techniques that has attracted global interest in the past decade. Research on GSI based on rubber-soil mixtures (RSM) has focused on structural performance under earthquake actions, whilst there are concerns over the serviceability limit states (SLS) requirements in relation to (i) human comfort under strong winds and (ii) ground settlement under gravity, which may induce cracking and durability issues in structures. This article presents the first study on the serviceability performance of buildings constructed with the GSI-RSM system. The finite element model of a coupled soil-foundation-structure system has been validated by data recorded from geotechnical centrifuge testing. The numerical estimates of ground settlement have also been compared with analytical predictions. It is concluded that the GSI-RSM system can satisfactorily fulfill the SLS requirements.

ARTICLE HISTORY
Received 3 April 2023
Accepted 21 June 2023

KEYWORDS
Geotechnical seismic isolation (GSI); Rubber-soil mixtures (RSM); Serviceability limit states (SLS); human comfort; wind; ground settlement

1. Introduction

Recent earthquakes have highlighted the importance of the resilience of our buildings and infrastructure. This promotes the adoption of low-damage seismic design strategies, such as base isolation and energy dissipation systems. There have also been developments of new techniques surrounding this theme, and one of which is geotechnical seismic isolation (GSI), which is a category of base isolation systems that are in direct contact with geomaterials and of which the isolation mechanism primarily involves geotechnics (Tsang 2009). A brief review of GSI techniques can be found in Tsang (2023) and the latest research and development can be found in the preface for the special issue on GSI published by the Bulletin of Earthquake Engineering (Tsang and Pitilakis 2023).

The use of rubber-soil mixtures (RSM) as a GSI foundation material, originally proposed by Tsang (2008), is the most researched (Abdullah and Hazarika 2016; Akhtar and Tsang 2023; Aloisio et al. 2023; Bernal-Sanchez, Leak, and Barreto 2023; Brunet, De la Llera, and Kausel 2016; Chiaro et al. 2023; Forcellini and Alzabeebee 2023; Kaneko et al. 2013; Pitilakis et al. 2021; Pitilakis, Karapetrou, and Tsagdi 2015; Tsang et al. 2009, 2012, 2021; Vratsikidis and Pitilakis 2023; Xiong and Li 2013; Xue et al. 2021). The GSI-RSM system exploits the beneficial effects of seismic soil-foundation-structure interaction. RSM has a lower modulus that reduces the lateral and rocking stiffness between the structure and the subsoil. Hence, the seismic response would be concentrated in the RSM layer, such that the demand on the superstructure can be reduced. This isolation mechanism has been illustrated via the use of a lumped-parameter analytical model (Tsang and Pitilakis 2019) and confirmed by a geotechnical centrifuge test (Tsang et al. 2021). Other advantages of the GSI-RSM system are the low cost, ease of implementation and the beneficial use of the huge stockpile of waste rubber tyres (Hernández et al. 2020; Tsang 2012). Apart from RSM, other materials, such as EPS beads (Edinçliler and Yildiz 2023), EPS geofoam (Karatzia and Mylonakis 2017), nylon fibres (Shimamura 2012) and super-absorbent polymers (SAP) (Nappa et al. 2016) have been explored and the concept of lateral disconnection (Somma et al. 2022) has been investigated. Other GSI mechanisms, such as sliding (Banović et al. 2023; Banović, Radnić, and Grgić 2019; Yegian and Catan 2004; Yegian and Kadakal 2004) and wave screening or scattering (Gatto et al. 2020, 2021; Gatto, Lentini, and Montrasio 2023; Nikitas and Bhattacharya 2023; Somma and Flora 2023) have also been investigated.

Research efforts have been put into the performance of GSI-RSM systems for protecting buildings and underground structures via numerical modelling, physical experiments and field testing. The changes in dynamic properties of the soil-foundation-structure system subjected to strong earthquake actions have been quantified, whilst performance indicators are mainly associated with

CONTACT Hing-Ho Tsang htsang@swin.edu.au School of Engineering, Swinburne University of Technology, Melbourne, Australia

roof acceleration, inter-storey drift, flexural stress and strain, as well as lateral force and overturning moment under earthquake actions.

Despite the proven effectiveness of GSI-RSM in structural demand reduction, concerns over the practicality and life-cycle serviceability (non-seismic) performance remain (Hooley and Al-Deen 2020; Parackal, Ginger, and Eaton 2022), which is reasonably expected for any new technology in the civil engineering industry. Due to the low modulus of the RSM foundation materials, one of the major concerns is related to the possibly excessive lateral deflection or vibrations of the building under strong wind situations that could compromise human comfort or damage non-structural components. Another major concern is the potential to experience excessive ground settlement due to gravity, because of poor compaction of the RSM layer due to the presence of elastic rubber particles, which can induce cracking and durability issues to the foundation and building structures. This study attempts to address these two issues. The results can also be a useful reference for GSI systems that are founded on other soft materials.

To overcome the high flexibility of the RSM layer, there have been excellent attempts to introduce geotextiles/geogrids (Anbazhagan, Manohar, and Divyesh 2015; Dhanya, Boominathan, and Banerjee 2020, 2022) for enhancing the stiffness and bearing capacity of the foundation soil. Also, a pile foundation can be provided to prevent ground settlement and ensure stability (Tsang et al. 2012). Whilst these measures can undoubtedly reduce ground deformation, they may, however, increase the complexity of construction or even compromise the isolation effectiveness as the fundamental mechanism of the GSI-RSM system is exactly based on the lower stiffness of the RSM layer for both horizontal and rocking responses. Hence, a balanced point needs to be found between desirable isolation effectiveness and an acceptable amount of ground settlement. It would be ideal if the amount of ground settlement of GSI-RSM systems without stiffening is already well below the allowable limit.

A numerical approach was adopted in this study to examine the two key serviceability requirements, namely, (i) human comfort under strong winds and (ii) permanent ground settlement under gravity. Section 2 describes the coupled soil-foundation-structure model, which has been carefully validated, in terms of the input shear modulus reduction curves, the fundamental natural period and Rayleigh damping of the models, and the characteristics of system response, based on the data recorded from the geotechnical centrifuge tests conducted by the authors and their collaborators (Tsang et al. 2021). Dynamic analysis using the validated numerical model based on simulated wind velocity time series was conducted (Section 3). Ground settlements have then been estimated in Section 4 and a comparison has been made with predictions from well-established analytical models.

2. Numerical model and experimental validation

2.1. Coupled soil-foundation-structure model

PLAXIS 2D was chosen for modelling the soil–structure interaction of the GSI-RSM system in this study. PLAXIS 2D is a two-dimensional finite element analysis software primarily for modelling a wide range of geotechnical engineering problems including both static and dynamic conditions. It has been widely adopted to simulate experiments conducted in a geotechnical centrifuge (Fasano et al. 2021; Manzari et al. 2018; Miranda, Nappa, and Bilotta 2019). It can model the building structure, its foundation system and the underlying soil sediments as a coupled system. Material models for subsoils can be accurately calibrated using experimental data. It also allows the incorporation of external loads to simulate the effects of wind pressures. The vibrational response of the coupled system can be calculated in the time domain.

The reference case study building model being considered is the same as the one adopted recently in the geotechnical centrifuge test (Tsang et al. 2021). The prototype structure is a realistic 15-m tall, five-storey reinforced concrete (RC) building with a plan of 18 m by 12 m, as low-to-medium-rise structures are considered suitable candidates for the use of the GSI-RSM technology (Tsang et al. 2012). A three-storey building model and an eight-storey building model were also used in a parametric study on different building heights and weights. Buildings with more than eight storeys are likely sitting on deep foundations, for which the two serviceability requirements are unlikely to be an issue. The two extra models are built based on the same structural elements as in the five-storey building model as shown in Figure 1.

The reference thickness of the RSM foundation layer below the building was chosen as 2 m, which is also the same as that in the centrifuge test (Tsang et al. 2021), whilst thicknesses of 1 m and 3 m were also considered in some cases for a parametric study. RSM with 30% rubber by weight (RSM-30%) was found in previous studies to be a desirable mix for use as GSI surrounding the building foundation (Tsang and Pitilakis 2019; Tsang et al. 2021). In this study, the natural soil (NS) material considered is clean gravel (with less than 5% fines), which is poorly graded with the D_{50} value of 7.3 mm, whilst the D_{50} value of rubber granules is 3.1 mm. A D_{50} ratio of around 0.4 was found to provide excellent seismic isolation (Brunet, De la Llera, and Kausel 2016).

The finite element model of the coupled soil-foundation-structure system is shown in Figure 1. The width of the sub-soil model (60 m) is set to be eight times the model thickness (7.5 m), to

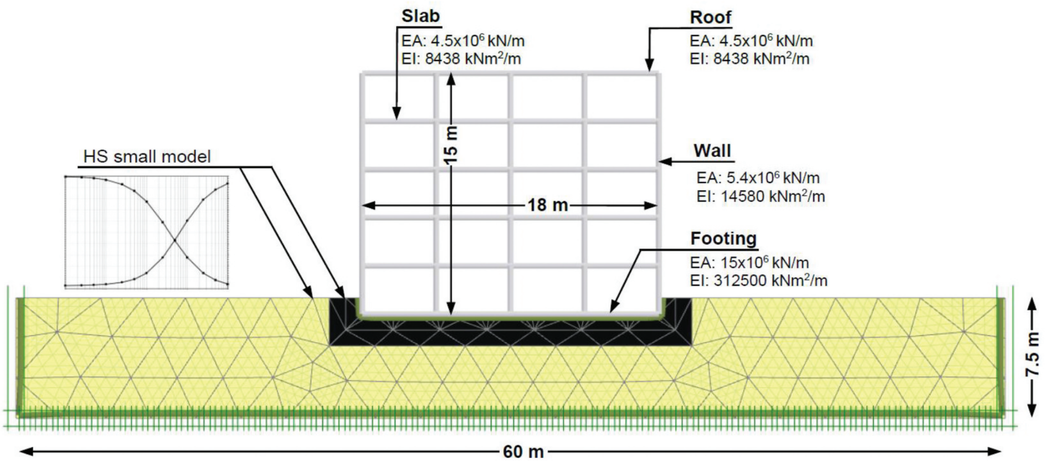

Figure 1. Coupled soil-foundation-structure finite element model of a five-storey reinforced concrete (RC) frame building with geotechnical seismic isolation (GSI) system based on rubber-soil mixtures (RSM) developed in PLAXIS 2D.

minimise the effects of boundary conditions in dynamic analyses (Amorosi, Boldini, and Falcone 2014). A larger thickness is not necessary as the sub-soil deformation decreases rapidly against depth. By using Boussinesq's equation to compute the variation in stress against depth z, the stress at z = 7.5 m (i.e. the base of the model) is only 1.8% of that at z = 1 m. Considering the shear modulus of RSM of 5 MPa at the upper 2 m, which is underlaid by natural soil (NS) with a shear modulus of 78 MPa, the strain at z = 7.5 m would just be 0.11% of that at z = 1 m, which is negligible.

15-node triangular plane-strain elements were selected to accurately model soil deformation. The global coarseness of the finite element mesh is set to obtain an accurate wave propagation by ensuring that the node spacing of soil elements is smaller than the wavelength of the predominant frequency component (3 Hz) of the input motions adopted for model calibration in the current study.

Different boundary conditions are specified for static and dynamic analysis. For settlement estimation, nodes along lateral sides are restrained in the horizontal direction only, so that vertical movement and deformation of soil at the boundaries are allowed under gravity. The base of the model is fully restrained in both horizontal and vertical directions mimicking the underlying bedrock. When input ground motions are applied at the base of the model for calibrating soil properties, viscous boundaries are employed on lateral sides to inhibit wave reflection into the soil body.

For the evaluation of serviceability against vibrations of buildings, it is assumed in the International Standard ISO 10137:2007 that the building structure does not yield or is not subject to non-linear effects. Hence, the material models used for the building structure are linear elastic.

2.2. Hardening soil model with small-strain stiffness (HS small model)

The hardening soil (HS) model is a commonly adopted constitutive model formulated based on the classical theory of plasticity for simulating the nonlinear behaviour of soils (Schanz, Vermeer, and Bonnier 1999). This is widely used by researchers to investigate soil deformations (Amorosi, Boldini, and Falcone 2014; Hejazi, Dias, and Kastner 2008; Höfle, Fillibeck, and Vogt 2008). The HS small model is extended from the HS model to properly consider small-strain soil stiffness and non-linear dependency on the strain γ that is also the strength of the HS small model compared to other constitutive models (Hejazi, Dias, and Kastner 2008).

RSM exhibits nonlinear response behaviours which are greatly influenced by the confining stress; hence, the HS small model is a suitable candidate as it can mimic the strain-dependent nonlinear behaviour of RSM, based on two input parameters, namely, small-strain shear modulus G_0 and shear strain level $\gamma_{0.7}$ when the secant shear modulus G is approximately 72.2% of G_0. Meanwhile, the hyperbolic shear modulus reduction function, which was developed based on Hardin and Drnevich (1972), adopted in this numerical study can be expressed as:

$$\frac{G}{G_0} = \frac{1}{1 + 0.385\left|\frac{\gamma}{\gamma_{0.7}}\right|} \tag{1}$$

The derivative of Equation (1) with respect to shear strain results in the tangent shear modulus G_t that is bounded by a lower limit at large-strain levels. The lower cut-off of G_t is introduced as the unloading-reloading shear modulus G_{ur}, which can be related to the unloading-reloading elastic modulus E_{ur} and the Poisson's ratio υ_{ur}:

$$G_t \geq G_{ur} = \frac{E_{ur}}{2(1 + \upsilon_{ur})} \tag{2}$$

Two other modulus parameters, E_{50} and E_{oed}, as defined in Table 1 for a reference confining pressure of 100 kPa, were obtained via a trial-and-error procedure to properly match the shear modulus reduction curve (refer to Section 2.3.2). A lower value of G_{ur}/G_0 represents a softer soil type with a higher damping ratio.

Furthermore, the shear modulus increases along soil depth as a stress dependency parameter which can be governed by the following equation:

$$G_0 = G_0^{ref}\left(\frac{c.\cos\phi + \sigma_1.\sin\phi}{c.\cos\phi + p^{ref}.\sin\phi}\right)^m \quad (3)$$

According to Equation (3), the small-strain shear modulus at a certain soil depth or stress level is a function of the confining pressure σ_1, strength parameters of cohesion c and friction angle ϕ at the reference confining pressure p^{ref} of 100 kPa and power for stress-level dependency m. Equation (3) expresses the stress dependency of shear modulus which is also similar to the stress dependency of Young's modulus under unloading and reloading stress path E_{ur}, the elastic modulus E_{50}, and the tangent modulus E_{oed}, respectively.

In this study, the HS small model for RSM was validated by using the data recorded from a recent dynamic centrifuge test conducted by the authors and their collaborators on the GSI-RSM system (Tsang et al. 2021). It is assumed that the water table is below the entire model, hence, dry condition is adopted. The key input parameters of the HS small model are summarised in Table 1.

2.3. Model validation based on geotechnical centrifuge data

2.3.1. Natural periods and Rayleigh damping models

For validating the HS small model of both NS and RSM foundation materials, a single-storey frame model, consistent with the one adopted in the centrifuge test reported in Tsang et al. (2021), was created in PLAXIS 2D. The fundamental natural period of the fixed-base single-storey model is equal to 0.85 s and its Rayleigh damping coefficient has been calibrated such that its damping ratio is 0.95% as measured during free vibrations in the hammer impact test. This structural damping level is consistent with the recommended maximum value of 1% for serviceability limit states of both steel and RC structures in AS/NZS 1170.2:2021. Based on the calibrated fixed-base model, the fundamental natural period of the flexible-base single-storey model sitting on NS and RSM is 0.90 s and 1.10 s, respectively, which are within 3% discrepancies from the values measured during free vibrations in the centrifuge. Meanwhile, the Rayleigh models for NS and RSM materials underneath the single-storey model have been added and calibrated such that the system response has a damping ratio of 1.8% and 3.0%, respectively, at low-shaking levels, also measured in the centrifuge test.

Next, a five-storey RC building frame that has the same dynamic properties, in terms of the fundamental natural period and the damping ratio, as the single-storey model was developed in PLAXIS 2D. The Rayleigh damping coefficients of NS and RSM materials calibrated based on the single-storey-frame-soil model were then adopted for the sub-soils of the five-storey-structure-soil model. The same material properties were adopted for the three-storey-structure-soil model and the eight-storey-structure-soil model.

2.3.2. Strain-dependent shear modulus of sub-soils

The most important parameter that governs the serviceability performance of the GSI-RSM system is the shear modulus of RSM. Hence, it is essential to make sure that the numerical model adopted in this study can represent a realistic scenario. Based on the input parameters in Table 1, the shear modulus of NS and RSM at various shear strains could be obtained via virtual cyclic direct simple shear (CDSS) test that is supported by PLAXIS 2D. The calculated function for RSM as shown in Figure 2 is compared with the strain-dependent shear modulus curve obtained from Senetakis, Anastasiadis, and Pitilakis (2012).

Table 1. Input parameters of the Hardening Soil model with small-strain stiffness (HS small model) for both natural soil (NS) and rubber-soil mixtures with 30% rubber by weight (RSM-30%).

Parameters [unit]	Symbols	NS	RSM-30%
Dry unit weight (kN/m^3)	γ_{unsat}	16.5	11.4
Power for the stress-level dependency of stiffness	m	0.59	0.87
Elastic modulus when reaching 50% of maximum deviatoric stress at 100 kPa confining pressure [kN/m^2]	E_{50}^{ref}	48262	2430
Tangent modulus when axial stress reaches 100 kPa in oedometer test [kN/m^2]	E_{oed}^{ref}	48262	1944
Elastic modulus under unloading/reloading condition	E_{ur}^{ref}	144786	7289
Poisson's ratio [-]	υ_{ur}	0.25	0.35
Small-strain shear modulus at 100 kPa confining pressure [kN/m^2][a]	G_0^{ref}	141537	6842
Shear strain level where the secant shear modulus G is 72.2% of small-strain shear modulus G_0 [%]	$\gamma_{0.7}$	0.003045	0.020450
Friction angle [degree][b]	ϕ	55	44
Cohesion [kN/m^2]	c	1	25

[a]G_0 values were estimated based on Anastasiadis, Senetakis, and Pitilakis (2012) and supported by the data measured in the centrifuge test (Tsang et al. 2021).
[b]Friction angle (ϕ) values were calibrated and supported by the data obtained by Tasalloti et al. (2021).

The calculated shear modulus reduction function was also validated by the data recorded in the dynamic centrifuge tests (Tsang et al. 2021). A simplified layout of the model tested in the geotechnical centrifuge at National Central University in Taiwan is shown in Figure 3. The acceleration response histories were recorded at depths of 1 m and 2 m (in prototype scale) underneath the middle of the foundation base, from which the stress-strain response histories of the foundation materials can be computed based on the approach described in Zeghal and Elgamal (1994). Hence, the shear modulus of the foundation materials at various strain levels can be estimated. Figure 2 shows that the HS small model can capture the strain-dependent response behaviour of the foundation materials very well.

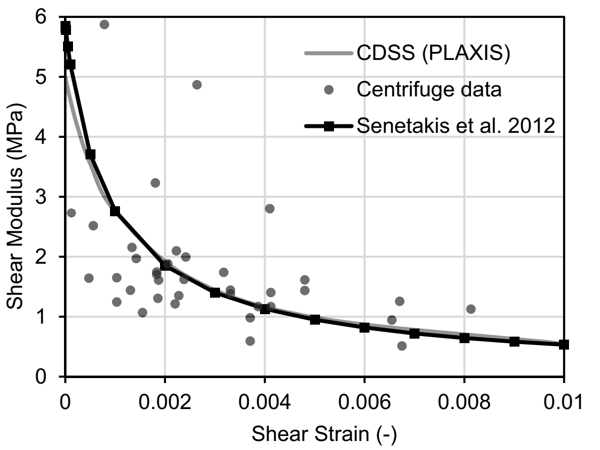

Figure 2. Validation of the HS small model for RSM (with 30% rubber by weight) based on a comparison of the shear modulus reduction curve obtained from the virtual cyclic direct simple shear (CDSS) test supported by PLAXIS 2D with that obtained from Senetakis, Anastasiadis, and Pitilakis (2012). and the data recorded in the dynamic centrifuge tests (Tsang et al. 2021).

2.3.3. Acceleration response of sub-soil

Once the most influential properties of the foundation materials has been validated, it would be prudent to examine the response at a critical location of the GSI-RSM system, to gain further confidence in the whole numerical model. For this purpose, the acceleration response at 1 m depth (in prototype scale) underneath the middle of the foundation base was selected.

A small-amplitude sinusoidal wave was applied by the shaker in the centrifuge, and the acceleration response at 1 m depth (in prototype scale) was recorded. The same input wave was applied in the numerical model, and the soil response at the same location was taken for a comparison in Figure 4. Close matches in both time and frequency domains are observed, and hence, the numerical model in PLAXIS was validated.

3. Human comfort in strong winds

Scepticism towards new technologies is not uncommon, especially in civil engineering. There were deep concerns over the use of prestressing, high-strength concrete, and traditional seismic isolation based on discrete bearings, just to name a few. These inventions result in more slender structures that are more dynamically responsive. Meanwhile, the increasing demand for human comfort and proper functioning of the facilities poses additional design requirements. GSI is no exception, and hence, there is a need to carefully examine the acceptability of vibrations in structures that are sitting on compressible foundation materials with respect to human response in daily living conditions.

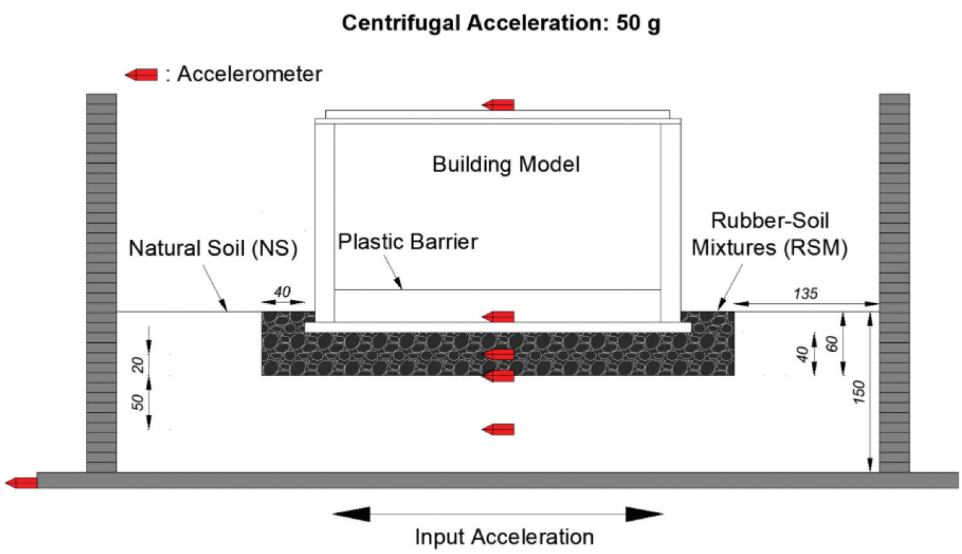

Figure 3. A simplified layout of the model tested in the geotechnical centrifuge at National Central University in Taiwan (Tsang et al. 2021) (dimensions in mm).

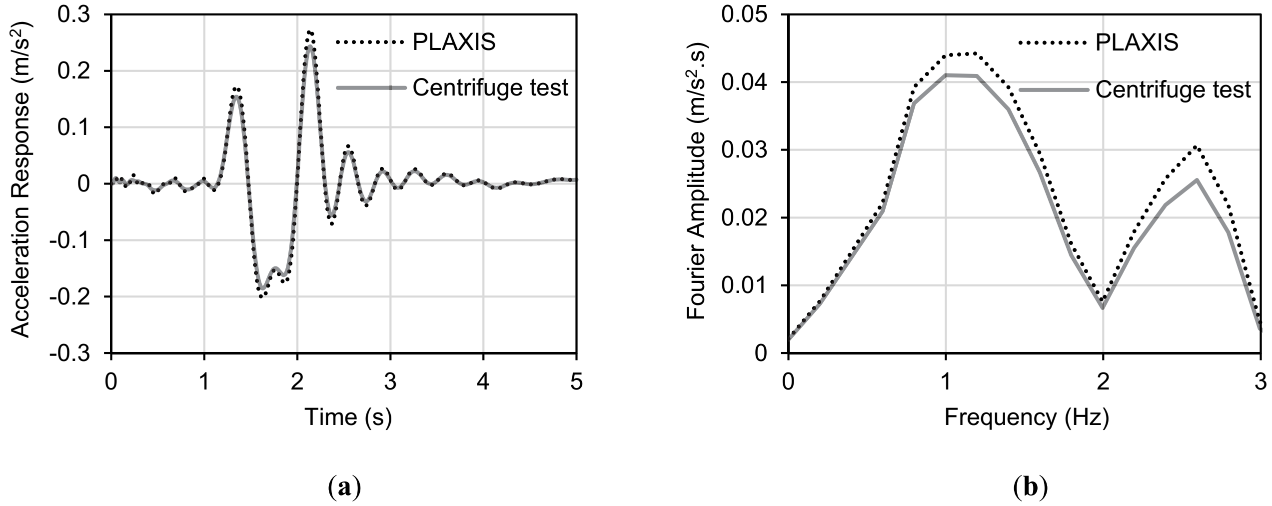

Figure 4. Validation of the HS small model for RSM (with 30% rubber by weight) based on a comparison of (a) the acceleration response time series and (b) the corresponding Fourier amplitude spectra at 1 m depth underneath the middle of the foundation base, simulated by PLAXIS 2D and those recorded in the dynamic centrifuge tests (Tsang et al. 2021).

3.1. Serviceability limits of wind-induced vibration

The International Standard ISO 10137:2007 was specifically developed for providing recommendations on the evaluation of serviceability against vibrations of buildings and walkways within buildings. The SLS is mainly described by the vibration levels in terms of acceleration, in conjunction with frequency values. Three categories of receivers are considered in the standard, namely, human occupants, building contents, and building structures. As GSI is considered most suited for ordinary residential and office buildings, the comfort of regular human occupants would be the primary concern. Amongst possible vibration sources, both inside and outside a building, wind flow that exerts pressures (or forces) on the building surface can induce significant vibrations in the building and affect the comfort of occupants regularly. It is noted that the expected level of wind-induced vibrations would not lead to any damage to structural or non-structural elements.

The Annex D of ISO 10137:2007 provides guidance for the evaluation of human response and habitability to wind-induced motions in regular office and residential buildings under daily living conditions. Clause D.1.2 discusses the acceptable peak horizontal acceleration at the fundamental natural frequency of the building. Fig. D.1 gives the evaluation curves for wind-induced vibrations in buildings in a horizontal direction for a one-year return period. The acceptable limit is the lowest for fundamental natural frequencies between 1 Hz and 2 Hz, which is 0.06 m/s/s for office buildings and 0.04 m/s/s for residential buildings. The limits are increased in proportion for buildings with fundamental natural frequencies beyond 2 Hz. The limit for residential buildings is close to the 90% level of the perception probability. The limits in ISO 10137:2007 are more stringent than those in the National Building Code of Canada (NBCC) and the Commentary on the Australian Standard for wind loads AS/NZS 1170.2:2021. It is noted that the level of vibration below 0.10 m/s/s or even 0.15 m/s/s is not considered annoying (Chang 1973).

On the other hand, Section 2.3 and the Appendix C of the Australian Standard AS/NZS 1170.0 2002 provide guidance on the criteria for evaluating the serviceability of ordinary building structures. Among the types of design serviceability conditions and serviceability response of the structure being covered in the standard, the side sway of the whole building is the primary concern in our case. This can be assessed by checking the lateral deflection at the building roof based on a wind event with a return period of 25 years. A deflection limit of Height/500 has to be satisfied.

3.2. Simulated wind velocity time series

In strong winds, structural vibrations arise from the interaction between the time-varying wind pressure and the inertial properties of the building structure. Wind pressure is a function of wind velocity, which is a type of stationary random motion. As for most vibration problems, the applied actions can be characterised by amplitude, frequency content and duration. The design wind speed is characterised by the peak gust wind speed at a height of 10 m from the ground surface. For a return period of one year, a regional wind speed of 37 m/s has been estimated as the highest among populated cities in Australia and New Zealand, according to Table 3.1 in AS/NZS 1170.2:2021. Wellington, the capital city of New Zealand, is in that region, which is also located in an area of high seismicity, where the GSI-RSM system may be applied (Hernández et al. 2020). The corresponding wind speed for a return period of 25 years is 46 m/s. Site-specific multipliers for cardinal direction (=1.0), terrain/height (=0.83) and topography (=1.0) were applied in this study, and a typical shielding multiplier of 0.8 was adopted.

As stated in Eurocode 1 (EN 1991-1-4 2005), a realistic 10-min wind velocity time series is required for dynamic analysis. The frequency content of the time-varying wind velocity can be modelled using the normalised spectrum of von Karman (1948), which has been widely adopted in many studies, such as Holmes and Bekele (2021) and Thordal, Bennetsen, and Koss (2019). An example of the 10-min time series generated for the wind speed at a height of 10 m from the ground surface as shown in Figure 5(a) have a mean (time-averaged) wind speed of 20.3 m/s that can match the required turbulence intensity of 23.9% as outlined in AS/NZS 1170.2:2021. The calculated spectrum of the simulated time series illustrates a good match with the von Karman spectrum model, as shown in Figure 5(b).

3.3. Dynamic analysis and results

The Deaves and Harris (D-H) equilibrium model (Deaves and Harris 1978) was used to determine the mean wind-speed profiles along the height of the case study building models. Whilst Figure 5 shows the wind speed time series at a height of 10 m from the ground surface, it can be scaled for and applied at different heights. The corresponding wind pressure time series were then calculated for different heights of the case study buildings accordingly. The wind load distribution can be computed by considering the tributary area surrounding the node (beam-column joint) at each floor level, as shown in Figure 6 using the five-storey building model as an example. A time step of 0.01 s was used in the response history analysis considering the coarseness of the finite element mesh and the shear wave velocity of elements. A sensitivity study revealed that the structural response was not affected much by using smaller time steps.

Examples of time series of the acceleration response at the roof of the five-storey building models are shown in Figure 7. The maximum acceleration and displacement responses are recorded at the roof levels for all three case study buildings. The values of the peak acceleration responses induced by three different input wind speed time series are summarised in Table 2. It is found that all of the values are below the acceptable limit recommended by ISO 10137:2007, whilst there is no significant difference in the response values or the patterns amongst the three sets of results. This has demonstrated the robustness of the results. In general, the buildings with the GSI-RSM system experienced an average of 15% larger peak acceleration responses compared to those sitting on NS. Meanwhile, amongst all cases based on the wind loads with a return period of 25 years, the largest value of the maximum displacement responses is approximately 15.2 mm for the eight-storey building model, which is well below the deflection limit of Height/500 (i.e. 48 mm).

4. Ground settlement under gravity

Concerns over the low modulus of RSM stem from the usual challenges facing geotechnical engineers in dealing with natural soft soils, which increase the likelihood of experiencing large settlements during and after the construction of the buildings and infrastructure built on them. These large settlements may induce unexpected deformations in the structure that could

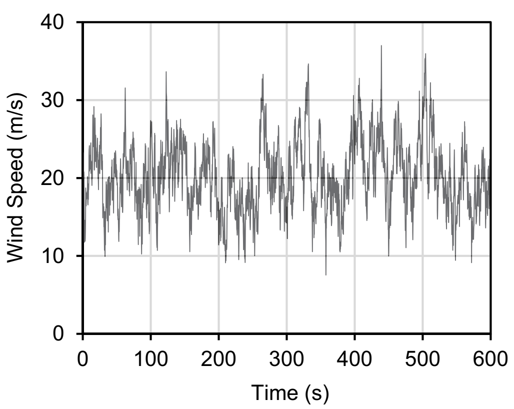

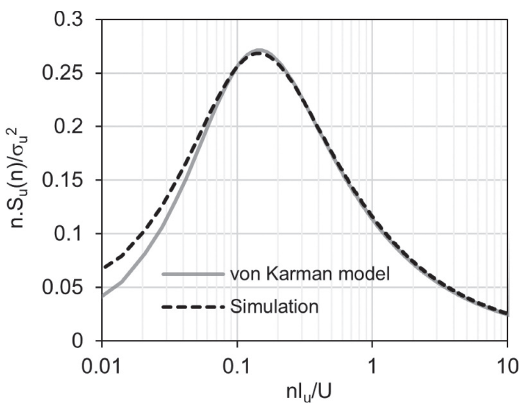

Figure 5. (a) an example of the 10-minute time series of wind speed stochastically generated based on (b) the normalised spectrum of von Karman (1948), that was applied at a height of 10 m from the ground surface of the five-storey case study building model. (S_u = spectral density, n = frequency, U = mean wind speed, σ_u = standard deviation, l_u = turbulence length scale).

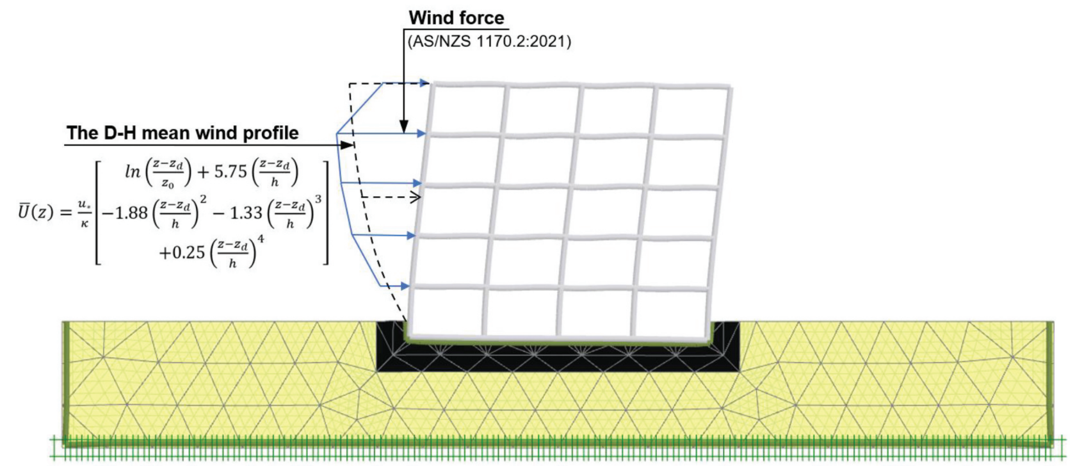

Figure 6. Finite element model of the five-storey case study building model constructed in PLAXIS 2D with the wind load profile based on the Deaves and Harris (D-H) equilibrium model (Deaves and Harris 1978) adopted in the response history analysis (noted that the deformation under the peak equivalent static wind load is magnified by 5000 times).

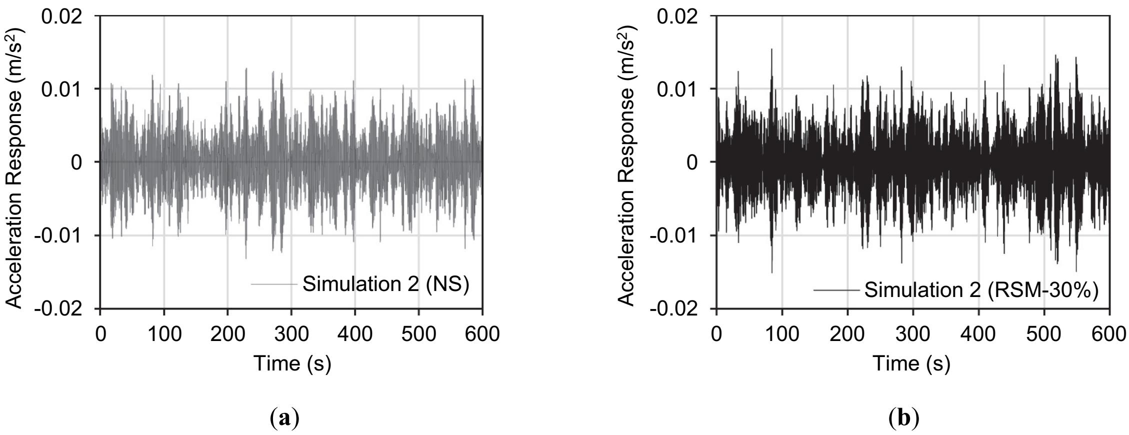

Figure 7. Time series of the acceleration response at the roof of the five-storey building models subjected to Wind Load Simulation 2: (a) Natural Soil (NS), and (b) RSM-30% (2 m).

Table 2. Peak acceleration responses (in the unit of m/s/s) at the roof of the case study buildings based on 1 m, 2 m and 3 m thick rubber-soil mixtures (RSM) induced by three different input wind speed time series for demonstrating the robustness of the results.

	Natural Soil (NS)	GSI-RSM (1 m)	GSI-RSM (2 m)	GSI-RSM (3 m)
3-storey				
Wind Load 1	0.006	0.008	0.008	0.007
Wind Load 2	0.006	0.008	0.007	0.007
Wind Load 3	0.009	0.008	0.008	0.006
5-storey				
Wind Load 1	0.014	0.018	0.019	0.019
Wind Load 2	0.013	0.014	0.015	0.016
Wind Load 3	0.014	0.016	0.016	0.015
8-storey				
Wind Load 1	0.027	0.030	0.029	0.030
Wind Load 2	0.025	0.031	0.030	0.030
Wind Load 3	0.025	0.030	0.030	0.032

impair its serviceability and function, and possibly lead to other durability and structural problems. However, there are indeed fundamental differences between typical natural soft soils and RSM. Whilst natural soft soils possess low shear strength, the addition of rubber granules into soils does not necessarily reduce shear strength and bearing capacity (Ahmad 1993; Attom 2006; Edil and Bosscher 1994; Edinçliler, Baykal, and Saygılı 2010; Ghazavi 2004; Zornberg, Cabral, and Viratjandr 2004). Also, the deformation of natural soft soils under loads is inelastic and irreversible, whilst RSM behaves more elastically and its deformation is reversible under earthquake shakings, as evidenced in the centrifuge test (Tsang et al. 2021).

4.1. Design limits of ground settlement

EN 1997, also known as Eurocode 7 (EN 1997–1:2004; EN 1997–2:2007), sets forth the design principles and requirements for safety and serviceability in relation to the geotechnical aspects of the design of buildings and civil infrastructure. Detailed design rules or models are given in the informative Annexes. Section 6 of Eurocode 7 Part 1 (EN 1997–1:2004) discusses various aspects of the design of foundations, including pad, strip, spread, raft and pile foundations. The Annex H in Part 1 of Eurocode 7 (EN 1997–1:2004) specifies the limiting values of structural deformation and foundation movement, in terms of the total permanent settlement, relative (or differential) settlement, angular distortion, and the like. Both serviceability and ultimate limit states for different types of structures are considered.

A maximum angular distortion of 1/500 and total permanent settlements of up to 50 mm are often accepted as the serviceability limits for many structures and utilities. Larger settlements are still considered acceptable provided that the angular distortion is within acceptable limits. For frame buildings and reinforced load-bearing walls, an angular distortion of 1/1000 to 1/1400 at end bays needs to be checked to avoid cracking in walls and partitions. Structural damage is not expected for an angular distortion below 1/250. For structures with unreinforced load-bearing walls, an angular distortion of 1/2500 is taken as the serviceability limit. Section 4.6.4.3(3) in Part 2 of Eurocode 7 (EN 1997–2:2007) states a recommended limiting value of 25 mm as the maximum total settlement for the allowable bearing resistance of sand.

4.2. Numerical estimates of ground settlement

A five-storey and an eight-storey RC building frames have been built in the PLAXIS platform through the procedure described in Section 2. For estimating permanent ground settlement, the contact pressure between the shallow foundation and the sub-soil is one of the determining factors. Iteration was required to calibrate and mimic the contact pressure of around 59 kPa and 90 kPa, respectively, induced by the five-storey and eight-storey building, based on a ballpark value of 10 kPa from each floor, as commonly adopted for preliminary design in engineering consulting offices. An example of the ground and structural deformation under the gravity of a five-storey building sitting on RSM of 2 m thick can be seen in Figure 8.

As summarised in Table 3, the numerical modelling indicates that the ground settlement is significantly increased when 30% rubber (by weight) is added into NS (pure gravel in this study). Nevertheless, all the values are far below the limit of 25 mm recommended by Eurocode 7 (EN 1997–1:2004; EN 1997–2:2007). Even for the most onerous scenario when an eight-storey building is sitting on RSM (30% by weight) of 3 m thick, the ground settlement is less than 8 mm, which has a wide margin from the code limits. On the other hand, the largest angular distortion amongst all scenarios is 1/8700, which is far below the code limits too.

4.3. Analytical estimates of ground settlement

Various analytical models have been developed over the past few decades for estimating the settlement of a foundation sitting on clay or sand deposits (Bowles 1987; Mayne and Poulos 1999; Schmertmann, Hartman, and Brown 1978; Skempton and Bjerrum 1957). Skempton and Bjerrum (1957) conducted an analysis of the immediate settlement of cohesive materials based on the theory of elasticity. Schmertmann, Hartman, and Brown (1978) introduced a semi-empirical strain influence factor to estimate the foundation settlement of granular material. The proposed analytical formula also takes into account the depth of foundation embedment and creep in soil. Bowles (1987) developed another expression that consists of a shape factor and a depth factor for estimating the settlement of flexible foundations based on the theory of elasticity. More recently, to consider the rigidity and the depth of embedment of the foundation, as well as the variation of elastic modulus of soil against depth, Mayne and Poulos (1999) proposed an improved formula for estimating the elastic settlement at the centre of the foundation. A summary of the four analytical

Table 3. Estimates of permanent ground settlement for GSI systems with 1 m, 2 m and 3 m thick rubber-soil mixtures (RSM) from both numerical and analytical methods.

Unit: mm	PLAXIS 2D	Skempton and Bjerrum (1957)	Schmertmann, Hartman, and Brown (1978)	Bowles (1987)	Mayne and Poulos (1999)
5-Storey Building					
NS	1.2	0.6	0.7	1.3	1.7
RSM (1 m)	2.9	1.4	0.8	2.7	4.2
RSM (2 m)	3.9	2.5	2.3	4.6	6.6
RSM (3 m)	4.7	3.9	4.2	6.8	8.9
8-Storey Building					
NS	1.8	0.9	1.1	1.9	2.6
RSM (1 m)	4.2	2.1	1.3	4.0	6.2
RSM (2 m)	5.9	3.8	3.5	6.8	9.7
RSM (3 m)	7.3	5.8	6.3	10.1	13.2

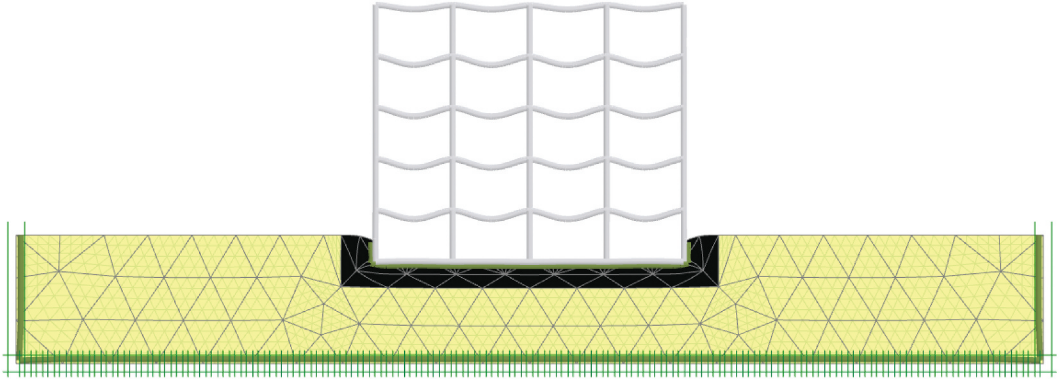

Figure 8. Ground and structural deformation under the gravity of a five-storey building sitting on RSM of 2 m thick (noted that the deformation is magnified by 120 times).

models for estimating foundation settlement is given in Table 4.

These models are simple-to-use and sufficient for routine engineering design. The results obtained from the numerical approaches in the previous sub-section can be verified by comparison with analytical estimates. It can be seen from Table 3 that the analytical estimates vary quite significantly among themselves, possibly due to the different materials considered in their studies and the different assumptions made in the development process. The numerical results are in the same order of magnitude as those analytical estimates and fall somewhat in the middle of the ranges. Hence, the numerical results are deemed to be credible.

Furthermore, the analytical model that provides the closest matches with the numerical results can be recommended for estimating the maximum ground settlement of GSI-RSM systems. It is found that, on average, Bowles (1987) model gives the best matches with the results from PLAXIS 2D and tends to give more conservative values for more flexible ground. The percentage difference between them is up to 45%, which is considered acceptable given the high variabilities of soil properties generally. Mayne and Poulos (1999) model generally gives larger values, which can be taken as a more conservative model for estimating ground settlement. The results indicate that ground settlement should not be a concern for the use of RSM for GSI, at least for typical buildings and GSI configurations, such as those considered in this study.

Table 4. Summary of the four analytical models for estimating permanent ground settlement.

Model	Formula	Definitions of parameters
Mayne and Poulos (1999)	$S_e = \frac{q_0 B_e I_G I_F I_E}{E_0}\left(1-\mu_s^2\right)$	q_0: applied pressure on the foundationl I_G: influence factor for variation of elastic modulus of foundation material I_F: foundation rigidity correction factor I_E: foundation embedment correction factor B_e: equivalent dimension of foundation as a circular foundation E_0: elastic modulus of foundation material at the bottom of foundation μ_s: Poisson's ratio of foundation material
Bowles (1987)	$S_e = q_0(\alpha B')\frac{1-\mu_s^2}{E_s} I_s I_f$	α: correction factor taking into account the location of settlement E_s: average modulus of elasticity of foundation material from the surface to about a depth equal to five times foundation width B': half of foundation width I_s: shape factor defined by Steinbrenner (1934) I_f: depth factor defined by Fox (1948)
Schmertmann, Hartman, and Brown (1978)	$S_e = C_1 C_2(\bar{q}-q)\sum_0^{Z_2}\frac{I_z}{E_s}\Delta z$	I_z: strain influence factor C_1: correction factor for embedment depth C_2: correction factor for creep in soil $\bar{q}$: applied pressure on the foundation q: effective stress caused by soil excavated
Skempton and Bjerrum (1957)	$S_e = qb\frac{3}{4E}I_p$	I_p: appropriate influence value defined by Steinbrenner (1934) b: width of the foundation E: elastic modulus of foundation material

5. Conclusions and closing remarks

Rubber-soil mixtures (RSM) have been extensively researched as a green material for large-volume consumptions in sustainable building construction and infrastructure projects. Surrounding the building foundation by RSM to create a geotechnical seismic isolation (GSI) system is a promising approach to enhancing the earthquake resilience of structures. This study attempted to address the concerns over the serviceability (non-seismic) performance of buildings, namely, human comfort under strong winds and permanent ground settlement under gravity. To this end, a numerical approach was adopted.

The finite element model of a coupled soil-foundation-structure system has been carefully validated by data recorded from geotechnical centrifuge testing (Section 2). Dynamic analysis using the validated numerical model based on simulated wind velocity time series was conducted (Section 3). It is found that the buildings with the GSI-RSM systems experienced an average of 15% larger peak acceleration responses compared to those sitting on natural soil (NS). However, all the computed structural responses are below the acceptable limit recommended by ISO 10137:2007.

Ground settlements have then been estimated using the validated numerical model and a comparison has been made with predictions by well-established analytical models (Section 4). The results indicate that the ground settlement is significantly increased when 30% rubber (by weight) is added. Nevertheless, all the values are far below the limit of 25 mm recommended by Eurocode 7 (EN 1997–1:2004; EN 1997–2:2007). Also, the analytical models of Bowles (1987) and Mayne and Poulos (1999) are recommended as suitable hand-calculation design tools for estimating the maximum ground settlement of buildings founded on RSM.

Given the large buffer from the recommended limit in Eurocode 7 (EN 1997–1:2004; EN 1997–2:2007), softer foundation materials can be used if they can enhance soil-foundation-structure interaction and isolation effectiveness. On the other hand, by replacing the top 1 m to 3 m of the original soil with well-controlled RSM, the uncertainties in terms of the foundation soil properties can be reduced and hence unexpected situations like excessive, differential or non-uniform settlement can be avoided. Also, it would not be a critical issue if the deformation is uniform across the whole RSM layer.

Nevertheless, there are other measures if one wants to keep the ground settlement to the minimum. It is found that the compressibility decreases substantially once tyre shreds have been loaded once (Edil and Bosscher 1994). Preloading or compaction can be performed to reduce compressibility. Also, the amount of settlement can be taken into account in the design stage with the current knowledge acquired through the extensive research that has been carried out in the past decade to characterise and quantify the deformability of RSM.

Acknowledgements

The support provided by Professor Wen-Yi Hung from National Central University in Taiwan for the geotechnical centrifuge testing is gratefully acknowledged. Feedback provided by Professor Kyriazis Pitilakis from Aristotle University of Thessaloniki in Greece on the draft manuscript is also acknowledged. This study is a part of the PhD project conducted by the second author, who is financially supported by the Bushfire and Natural Hazards Cooperative Research Centre and the Swinburne University Postgraduate Research Award.

Disclosure statement

No potential conflict of interest was reported by the author(s).

ORCID

Hing-Ho Tsang http://orcid.org/0000-0002-4912-5184

Data availability statement

Data are available on request from the authors.

References

Abdullah, A., and H. Hazarika. 2016. "Improvement of Shallow Foundation Using Non-Liquefiable Recycle Materials." *Japanese Geotechnical Society Special Publication* 2 (54): 1863–1867. https://doi.org/10.3208/jgssp.SEA-08.

Ahmad, I. 1993, "Laboratory Study on Properties on Rubber soils", Report No. FHWA/IN/JHRP-93/4, Joint Highway Research Project, Indiana Department of Transportation, USA.

Akhtar, A. Y., and H. H. Tsang. 2023. "Dynamic Properties of Recycled Polyurethane-Coated Rubber-Soil Mixtures." *Case Studies in Construction Materials* 18:e01859. https://doi.org/10.1016/j.cscm.2023.e01859.

Aloisio, A., A. Contento, J. Xue, R. Fu, M. Fragiacomo, and B. Briseghella. 2023. "Probabilistic Formulation for the Q-Factor of Piles with Damping Pre-Hole." *Bulletin of Earthquake Engineering* 21 (8): 3749–3775. https://doi.org/10.1007/s10518-022-01497-7.

Amorosi, A., D. Boldini, and G. Falcone. 2014. "Numerical Prediction of Tunnel Performance During Centrifuge Dynamic Tests." *Acta Geotechnica* 9 (4): 581–596. https://doi.org/10.1007/s11440-013-0295-7.

Anastasiadis, A., K. Senetakis, and K. Pitilakis. 2012. "Small-Strain Shear Modulus and Damping Ratio of Sand-Rubber and Gravel-Rubber Mixtures." *Geotechnical and Geological Engineering* 30 (2): 363–382. https://doi.org/10.1007/s10706-011-9473-2.

Anbazhagan, P., D. R. Manohar, and R. Divyesh. 2015. "Low Cost Damping Scheme for Low to Medium Rise

Buildings Using Rubber Soil Mixtures." *Japanese Geotechnical Society Special Publication* 3 (2): 24–28. https://doi.org/10.3208/jgssp.v03.i05.

AS/NZS 1170.0. 2002. *Australian/New Zealand Standard. Structural Design Actions. Part 0: General Principles.* Standards Australia and Standards New Zealand.

AS/NZS 1170.2:2021. Australian/New Zealand Standard. Structural Design Actions. Part 2: Wind Actions. Standards Australia and Standards New Zealand.

Attom, M. F. 2006. "The Use of Shredded Waste Tires to Improve the Geotechnical Engineering Properties of Sands." *Environmental Geology* 49 (4): 497–503. https://doi.org/10.1007/s00254-005-0003-5.

Banović, I., J. Radnić, and N. Grgić. 2019. "Geotechnical Seismic Isolation System Based on Sliding Mechanism Using Stone Pebble Layer: Shake-Table Experiments." *Shock and Vibration, Article ID* 2019:1–26. https://doi.org/10.1155/2019/9346232 .

Banović, I., J. Radnić, N. Grgić, and K. Semren. 2023. "Effectiveness of Several Low-Cost Geotechnical Seismic Isolation Methods: A Shake-Table Study." *Bulletin of Earthquake Engineering* 21 (8): 3923–3947. https://doi.org/10.1007/s10518-022-01481-1.

Bernal-Sanchez, J., J. Leak, and D. Barreto. 2023. "Rubber-Soil Mixtures: Use of Grading Entropy Theory to Evaluate Stiffness and Liquefaction Susceptibility." *Bulletin of Earthquake Engineering* 21 (8): 3777–3796. https://doi.org/10.1007/s10518-023-01673-3.

Bowles, J. E. 1987. "Elastic Foundation Settlement on Sand Deposits." *Journal of Geotechnical Engineering, ASCE* 113 (8): 846–860. https://doi.org/10.1061/(ASCE)0733-9410(1987)113:8(846).

Brunet, S., J. C. De la Llera, and E. Kausel. 2016. "Non-Linear Modeling of Seismic Isolation Systems Made of Recycled Tire-Rubber." *Soil Dynamics and Earthquake Engineering* 85:134–145. https://doi.org/10.1016/j.soildyn.2016.03.019.

Chang, F. K. 1973. "Human Response to Motions in Tall Buildings." *Journal of the Structural Division* 99 (6, Jun): 1259–1272. https://doi.org/10.1061/JSDEAG.0003537.

Chiaro, G., A. Palermo, L. Banasiak, A. Tasalloti, G. Granello, and E. Hernandez. 2023. "Seismic Response of Low-Rise Buildings with Eco-Rubber Geotechnical Seismic Isolation (ERGSI) Foundation System: Numerical Investigation." *Bulletin of Earthquake Engineering* 21 (8): 3797–3821. https://doi.org/10.1007/s10518-022-01584-9.

Deaves, D. M., R. I. Harris. 1978. Mathematical Model of the Structure of Strong Winds. Construction Industry Research and Information Association (CIRIA), Report Number 76, London, England, ISBN-13: 978-0860170860, 49 pp.

Dhanya, J. S., A. Boominathan, and S. Banerjee. 2020. "Response of Low-Rise Building with Geotechnical Seismic Isolation System." *Soil Dyn Earthq Eng* 136:106187. https://doi.org/10.1016/j.soildyn.2020.106187.

Dhanya, J. S., A. Boominathan, and S. Banerjee. 2022. "Investigation of Geotechnical Seismic Isolation Bed in Horizontal Vibration Mitigation." *Journal of Geotechnical and Geoenvironmental Engineering* 148 (12): 04022108. https://doi.org/10.1061/(ASCE)GT.1943-5606.0002917.

Edil, T. B., and P. J. Bosscher. 1994. "Engineering Properties of Tire Chips and Soil Mixtures." *Geotechnical Testing Journal* 17 (4): 453–464. https://doi.org/10.1520/GTJ10306J.

Edinçliler, A., G. Baykal, and A. Saygılı. 2010. "Influence of Different Processing Techniques on the Mechanical Properties of Used Tires in Embankment Construction." *Waste Management* 30 (6): 1073–1080. https://doi.org/10.1016/j.wasman.2009.09.031.

Edinçliler, A., and Ö. Yildiz. 2023. "Shaking Fig Tests on Geotechnical Seismic Isolation for Medium-Rise Buildings Using EPS Beads-Sand Mixtures." *Bulletin of Earthquake Engineering* 21 (8): 3851–3877. https://doi.org/10.1007/s10518-022-01587-6.

EN 1991-1-4:2005. Eurocode 1. Actions on structures. General actions. Wind actions.

EN 1997-1:2004. Eurocode 7: Geotechnical Design Part 1: General Rules.

EN 1997-2:2007. Eurocode 7: Geotechnical Design. Part 2: Ground Investigation and Testing. 202 pp. https://geotechnicaldesign.info/ec7p2.html.

Fasano, G., V. Nappa, A. G. Özcebe, and E. Bilotta. 2021. "Numerical Modelling of the Effect of Horizontal Drains in Centrifuge Tests on Soil-Structure Interaction in Liquefiable Soils." *Bulletin of Earthquake Engineering* 19 (10): 3895–3931. https://doi.org/10.1007/s10518-021-01084-2.

Forcellini, D., and S. Alzabeebee. 2023. "Seismic Fragility Assessment of Geotechnical Seismic Isolation (GSI) for Bridge Configuration." *Bulletin of Earthquake Engineering* 21 (8): 3969–3990. https://doi.org/10.1007/s10518-022-01356-5.

Fox, E. N. 1948. "The Mean Elastic Settlement of a Uniformly Loaded Area at a Depth Below the Ground Surface," Proceedings, 2nd International Conference on Soil Mechanics and Foundation Engineering, Rotterdam, Netherlands, Vol. 1, pp. 129–132.

Gatto, M. P. A., V. Lentini, F. Castelli, L. Montrasio, and D. Grassi. 2021. "The Use of Polyurethane Injection as a Geotechnical Seismic Isolation Method in Large-Scale Applications: A Numerical Study." *Geosciences* 11 (5): 201. https://doi.org/10.3390/geosciences11050201 .

Gatto, M. P. A., V. Lentini, and L. Montrasio. 2023. Dynamic properties of polyurethane from resonant column tests for numerical GSI study. *Bulletin of Earthquake Engineering* 21 (8): 3991–4017 . https://doi.org/10.1007/s10518-022-01412-0.

Gatto, M. P. A., L. Montrasio, M. Berardengo, and M. Vanali. 2020. "Experimental Analysis of the Effects of a Polyurethane Foam on Geotechnical Seismic Isolation." *Journal of Earthquake Engineering* 26 (6): 2948–2969. https://doi.org/10.1080/13632469.2020.1779871.

Ghazavi, M. 2004. "Shear Strength Characteristics of Sand-Mixed with Granular Rubber." *Geotechnical and Geological Engineering* 22 (3): 401–416. https://doi.org/10.1023/B:GEGE.0000025035.74092.6c.

Hardin, B., and V. Drnevich. 1972. "Shear Modulus and Damping in Soils: Design Equations and Curves." *Journal of the Soil Mechanics and Foundations Division* 98 (7): 667–692. https://doi.org/10.1061/JSFEAQ.0001760.

Hejazi, Y., D. Dias, and R. Kastner. 2008. "Impact of Constitutive Models on the Numerical Analysis of Underground Constructions." *Acta Geotechnica* 3 (4): 251–258. https://doi.org/10.1007/s11440-008-0056-1.

Hernández, E., A. Palermo, G. Granello, G. Chiaro, and L. J. Banasiak. 2020. "Eco-Rubber Seismic-Isolation Foundation Systems: A Sustainable Solution for the New Zealand Context." *Structural Engineering International* 30 (2): 192–200. https://doi.org/10.1080/10168664.2019.1702487.

Höfle, R., J. Fillibeck, and N. Vogt. 2008. "Time Dependent Deformations During Tunnelling and Stability of Tunnel Faces in Fine-Grained Soils Under Groundwater." *Acta Geotechnica* 3 (4): 309–316. https://doi.org/10.1007/s11440-008-0075-y.

Holmes, J. D., and S. Bekele. 2021. *Wind Loading of Structures*, 4th ed., 638. UK: CRC Press. ISBN: 9780367273262.

Hooley, I. W., and S. Al-Deen. 2020. "Design of Cantilever Retaining Walls for Minimum Tilting Tendency." *Australian Journal of Structural Engineering* 21 (3): 254–262. https://doi.org/10.1080/13287982.2020.1783068 .

ISO 10137:2007. Bases for Design of Structures - Serviceability of Buildings and Walkways Against Vibrations. International Organization for Standardization (ISO). 44 pp.

Kaneko, T., R. P. Orense, M. Hyodo, and N. Yoshimoto. 2013. "Seismic Response Characteristics of Saturated Sand Deposits Mixed with Tire Chips." *Journal of Geotechnical and Geoenvironmental Engineering (ASCE)* 139 (4): 633–643. https://doi.org/10.1061/(ASCE)GT.1943-5606.0000752.

Karatzia, X., G. Mylonakis. 2017. Geotechnical Isolation of Pile-Supported Bridge Piers Using EPS Geofoam. In: Proceedings of the 16th world conference on earthquake engineering, Santiago, Chile.

Manzari, M. T., M. E. Ghoraiby, B. L. Kutter, M. Zeghal, T. Abdoun, P. Arduino, R. J. Armstrong, et al. 2018. "Liquefaction Experiment and Analysis Projects (LEAP): Summary of Observations from the Planning Phase." *Soil Dynamics and Earthquake Engineering* 113:714–743. https://doi.org/10.1016/j.soildyn.2017.05.015.

Mayne, P. W., and H. G. Poulos. 1999. "Approximate Displacement Influence Factors for Elastic Shallow Foundations." *Journal of Geotechnical and Geoenvironmental Engineering ASCE* 125 (6): 453–460. https://doi.org/10.1061/(ASCE)1090-0241(1999)125:6(453).

Miranda, G., V. Nappa, and E. Bilotta. 2019. "Preliminary Numerical Simulation of Centrifuge Tests on Tunnel-Building Interaction in Liquefiable Soil." *Geotechnical Research for Land Protection and Development*, 583–591. Springer International Publishing.

Nappa, V., E. Bilotta, A. Flora, and S. P. G. Madabhushi. 2016. *Centrifuge Modelling of the Seismic Performance of Soft Buried Barriers*. Bull Earthq Eng. https://doi.org/10.1007/s10518-016-9912-9.

Nikitas, G., and S. Bhattacharya. 2023. "Experimental Study on Sand-Tire Chip Mixture Foundations Acting as a Soil Liquefaction Countermeasure." *Bulletin of Earthquake Engineering* 21 (8): 4037–4063. https://doi.org/10.1007/s10518-023-01667-1.

Parackal, K. I., J. D. Ginger, and J. Eaton. 2022. "Wind Loads on Double-Skillion Roof Houses." *Australian Journal of Structural Engineering* 23 (1): 26–36. https://doi.org/10.1080/13287982.2021.1997369.

Pitilakis, D., A. Anastasiadis, A. Vratsikidis, A. Kapouniaris, M. R. Massimino, G. Abate, and S. Corsico. 2021. "Large-Scale Field Testing of Geotechnical Seismic Isolation of Structures Using Gravel-Rubber Mixtures." *Earthquake Engineering & Structural Dynamics* 50 (10): 2712–2731. https://doi.org/10.1002/eqe.3468.

Pitilakis, K., S. Karapetrou, and K. Tsagdi. 2015. "Numerical Investigation of the Seismic Response of RC Buildings on Soil Replaced with Rubber–Sand Mixtures." *Soil Dynamics and Earthquake Engineering* 79:237–252. https://doi.org/10.1016/j.soildyn.2015.09.018.

Schanz, T., P. A. Vermeer, and P. G. Bonnier, "The Hardening Soil Model: Formulation and verification," in Beyond 2000 in Computational Geotechnics. Ten Years of PLAXIS International. Proceedings of the international symposium, Amsterdam, March 1999. 1999, pp. 281–296, https://doi.org/10.1201/9781315138206-27.

Schmertmann, J. H., J. P. Hartman, and P. R. Brown. 1978. "Improved Strain Influence Factor Diagrams." *Journal of the Geotechnical Engineering Division, American Society of Civil Engineers* 104 (GT8): 1131–1135. https://doi.org/10.1061/AJGEB6.0000683.

Senetakis, K., A. Anastasiadis, and K. Pitilakis. 2012. "Dynamic Properties of Dry Sand/Rubber (RSM) and Gravel/Rubber (GRM) Mixtures in a Wide Range of Shearing Strain Amplitudes." *Soil Dynamics and Earthquake Engineering* 33 (1): 38–53. https://doi.org/10.1016/j.soildyn.2011.10.003.

Shimamura, A. 2012. Study on Earthquake Response Reduction by Improved Composite Geo-material using Rubber Chips and Fibrous materials (translated from Japanese). PhD Thesis, Osaka University, Japan

Skempton, A. W., and L. Bjerrum. 1957. "A Contribution to the Settlement Analysis of Foundations on Clay." *Géotechnique* 7 (4): 168–178. https://doi.org/10.1680/geot.1957.7.4.168.

Somma, F., E. Bilotta, A. Flora, and G. M. B. Viggiani. 2022. "Centrifuge Modeling of Shallow Foundation Lateral Disconnection to Reduce Seismic Vulnerability." *Journal of Geotechnical and Geoenvironmental Engineering* 148 (2): 04021187. https://doi.org/10.1061/(ASCE)GT.1943-5606.0002746.

Somma, F., and A. Flora. 2023. "SAP-Sand Mixtures as a Geotechnical Seismic Isolation Technology: From the Dynamic Characterization to a Simple Analytical Design Approach." *Bulletin of Earthquake Engineering* 21 (8): 4065–4089. https://doi.org/10.1007/s10518-023-01660-8.

Steinbrenner, W. 1934. "Tafeln zur Setzungsberechnung." *Die Strasse* 1:121–124.

Tasalloti, A., G. Chiaro, L. Banasiak, and A. Palermo. 2021. "Experimental Investigation of the Mechanical Behaviour of Gravel-Granulated Tyre Rubber Mixtures Construction & Building Materials." *Construction and Building Materials* 273:121749. https://doi.org/10.1016/j.conbuildmat.2020.121749.

Thordal, M. S., J. C. Bennetsen, and H. H. H. Koss. 2019. "Review for Practical Application of CFD for the Determination of Wind Load on High-Rise Buildings." *Journal of Wind Engineering & Industrial Aerodynamics* 186 (Mar): 155–168. https://doi.org/10.1016/j.jweia.2018.12.019.

Tsang, H. H. 2008. "Seismic Isolation by Rubber–Soil Mixtures for Developing Countries." *Earthquake Engineering & Structural Dynamics* 37 (2): 283–303. https://doi.org/10.1002/eqe.756.

Tsang, H. H. 2009. "Geotechnical Seismic Isolation." In *Earthquake Engineering: New Research*, 55–87. New York: Nova Science Publishers Inc.

Tsang, H. H. 2012. "Uses of Scrap Rubber Tires." In *Rubber: Types, Properties and Uses*, 477–492. New York: Nova Science Publishers Inc.

Tsang, H. H. 2023. "Analytical Design Models for Geotechnical Seismic Isolation Systems." *Bulletin of Earthquake Engineering* 21 (8): 3881–3904. https://doi.org/10.1007/s10518-022-01469-x.

Tsang, H. H., J. Y. K. Lam, S. Yaghmaei-Sabegh, S. H. Lo. 2009. Protecting Underground Tunnel by Rubber–Soil Mixtures. In: Proceedings of the 7th International

Conference on Lifeline Earthquake Engineering, ASCE-TCLEE, Oakland, California, U.S.

Tsang, H. H., S. H. Lo, X. Xu, and M. N. Sheikh. 2012. "Seismic Isolation for Low-To-Medium-Rise Buildings Using Granulated Rubber–Soil Mixtures: Numerical Study." *Earthquake Engineering & Structural Dynamics* 41 (14): 2009–2024. https://doi.org/10.1002/eqe.2171.

Tsang, H. H., and K. Pitilakis. 2019. "Mechanism of Geotechnical Seismic Isolation System: Analytical Modeling." *Soil Dynamics and Earthquake Engineering* 122:171–184. https://doi.org/10.1016/j.soildyn.2019.03.037 .

Tsang, H. H., and K. Pitilakis. 2023. "Preface for the Special Issue on Geotechnical Seismic Isolation (GSI)." *Bulletin of Earthquake Engineering* 21 (8): 3745–3748. https://doi.org/10.1007/s10518-023-01694-y.

Tsang, H. H., D. P. Tran, W. Y. Hung, K. Pitilakis, and E. F. Gad. 2021. "Performance of Geotechnical Seismic Isolation System Using Rubber–Soil Mixtures in Centrifuge Testing." *Earthquake Engineering & Structural Dynamics* 50 (5): 1271–1289. https://doi.org/10.1002/eqe.3398 .

von Karman, T. 1948. "Progress in the Statistical Theory of Turbulence." *Proceedings of the National Academy of Sciences* 34:530–539.

Vratsikidis, A., and D. Pitilakis. 2023. "Field Testing of Gravel-Rubber Mixtures as Geotechnical Seismic Isolation." *Bulletin of Earthquake Engineering* 21 (8): 3905–3922. https://doi.org/10.1007/s10518-022-01541-6.

Xiong, W., and Y. Li. 2013. "Seismic Isolation Using Granulated Tire–Soil Mixtures for Less-Developed Regions: Experimental Validation." *Earthquake Engineering and Structural Dynamics* 42:2187–2193. https://doi.org/10.1002/eqe.2315.

Xue, J., A. Aloisio, Y. Lin, M. Fragiacomo, and B. Briseghella. 2021. "Optimum Design of Piles with Pre-Hole Filled with High-Damping Material: Experimental Tests and Analytical Modeling." *Soil Dynamics and Earthquake Engineering* 151 (106995): 106995. Article no. https://doi.org/10.1016/j.soildyn.2021.106995.

Yegian, M. K., and M. Catan. 2004. "Soil Isolation for Seismic Protection Using a Smooth Synthetic Liner." *Journal of Geotechnical and Geoenvironmental Engineering* 130 (11): 1131–1139. https://doi.org/10.1061/(ASCE)1090-0241(2004)130:11(1131).

Yegian, M. K., and U. Kadakal. 2004. "Foundation Isolation for Seismic Protection Using a Smooth Synthetic Liner." *Journal of Geotechnical and Geoenvironmental Engineering* 130 (11): 1121–1130. https://doi.org/10.1061/(ASCE)1090-0241(2004)130:11(1121).

Zeghal, M., and A.-W. Elgamal. 1994. "Analysis of Site Liquefaction Using Earthquake Records." *Journal of Geotechnical Engineering* 120 (6): 996–1017. https://doi.org/10.1061/(ASCE)0733-9410(1994)120:6(996).

Zornberg, J. G., A. R. Cabral, and C. Viratjandr. 2004. "Behaviour of Tire Shred - Sand Mixtures." *Canadian Geotechnical Journal* 41 (2): 227–241. https://doi.org/10.1139/t03-086.